COBEM 99
XV Congresso Brasileiro de Engenharia Mecânica
15th Brazilian Congress of Mechanical Engineering
22 - 26 de Novembro de 1999 / November 22 - 26, 1999 Águas de Lindóia, São Paulo,

CONTACT MECHANICS OF CERAMIC-COATED BEARINGS

Luiz A. de Lacerda
Luiz C. Wrobel
Brunel University, Department of Mechanical Engineering,
Uxbridge, Middlesex UB8 3PH, UK.

Abstract . *This paper presents a boundary element analysis of the contact mechanics between steel bearings with different ceramic coatings and thicknesses. The physical contact between the spherical bearings, and between the bearings and other components, makes the problem geometrically nonlinear such that an iterative procedure of solution is required. An efficient axisymmetric BEM formulation has been developed for this purpose which incorporates features such as subregion modelling and a fast iterative solver.*

Keywords: Boundary Element Method, Axisymmetry, Contact

1. INTRODUCTION

The useful life and reliability of mechanical components such as steel bearings can be improved by using protective overlay coatings of more resistant materials. This protection is fundamental to reduce wear at the surface of these non-conforming contact structures where localized high stress concentrations are usually found.

The lifetime of the coated body is certainly extended but conventional surface wear will no longer be the main reason for discarding the object. Detachment and fracture of the coating become the most frequent failure processes. Both stem from the combination of specific stresses and the coating properties.

Although intrinsic and thermal stresses are inherent from the coating manufacturing process, in the present work, stresses are restricted to those originated from the application of external loads. Also, linear elastic analysis and Coulomb friction law are adopted.

A few analytical methods for homogeneous contacting bodies exist, however, their application to layered materials is not appropriate. Chen (1971) and Gupta and Walowit (1974) developed numerical procedures using integral transforms for stress computation in layered media under specific conditions.

Djabella and Arnell (1992) used the Finite Element Method to analyse contact stresses in a single layer coated system. Despite using a powerful tool like FEM their contact model was of limited applicability since a Hertzian pressure distribution was employed to simulate the contact phenomena. Schwarzer *et al.* (1995) used a similar model and compared their results to available analytical solutions. Ahmed (1997) also

used FEM to perform a linear elastic frictionless contact analysis between two bearings, one of them being layered.

The Boundary Element Method is a suitable alternative technique to analyse linear elastic contact problems. It has two particular advantages over other methods: 1- only the boundaries need to be modelled; 2- required stresses are calculated with the same level of accuracy of displacements, an important feature when high stress gradients are present. Abdul-Mihsein *et al.* (1986) developed an axisymmetric boundary element formulation for contact mechanics and successfully analysed conforming and non-conforming contact problems. In the present study a similar formulation is used with subregions to model the different material layers. Also, an alternative load increment technique (Man *et al.*, 1993) is employed along with a fast solver routine (Ezawa & Okamoto, 1989).

2. AXISYMMETRIC BOUNDARY ELEMENT METHOD

Let the two-dimensional body B in Fig. 1 rotate 360 degrees about the z axis. An axisymmetric geometry under an axisymmetric load is formed where r and θ are the radial and hoop directions. All displacements and stresses are constant for any value of θ and this type of problem can be more efficiently analysed by simply considering the 2-D body B instead of the whole 3-D domain. As a result of this axisymmetry, directions r and z are sufficient to define the problem.

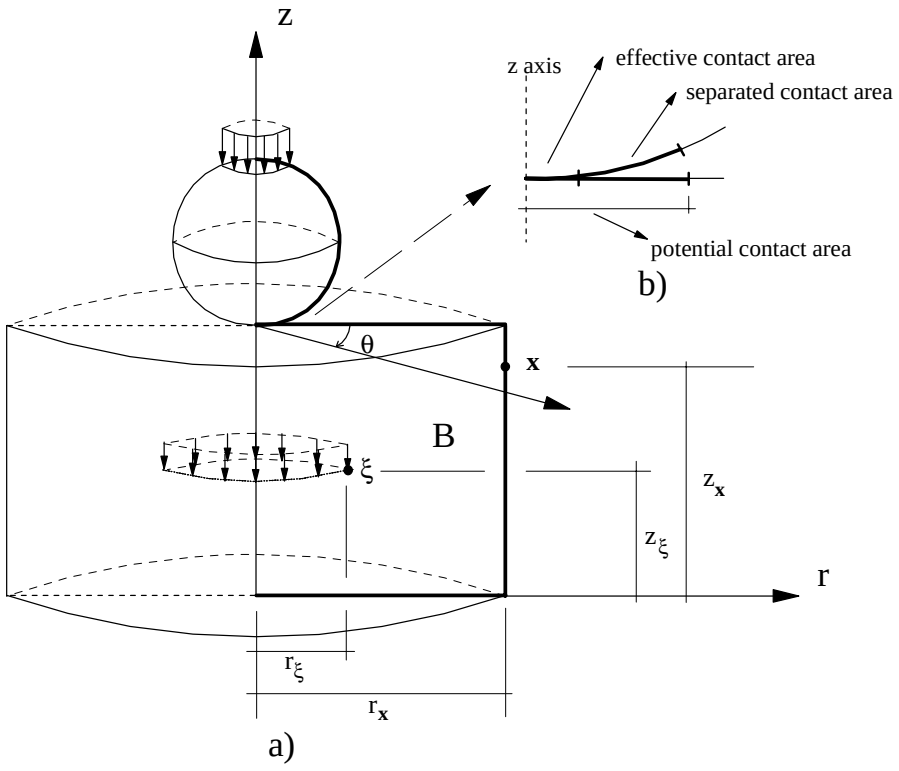

Figure 1: a) The axisymmetric problem representation and b) the potential contact area

The development of a boundary element formulation for this class of problem involves some algebraic manipulations and the result is comparable to a 2-D formulation with a more complex fundamental solution. One possible approach for deriving it consists on

transforming the 3-D BEM formulation from cartesian into cylindrical coordinates and integrating all terms with respect to the hoop direction (0 to 2π). A detailed discussion of this procedure and another possible approach has been presented by Becker (1986).

The axisymmetric boundary integral equation is of the form

$$\begin{bmatrix} C_{rr}(\boldsymbol{\xi}) & C_{rz}(\boldsymbol{\xi}) \\ C_{zr}(\boldsymbol{\xi}) & C_{zz}(\boldsymbol{\xi}) \end{bmatrix} \begin{bmatrix} u_r(\boldsymbol{\xi}) \\ u_z(\boldsymbol{\xi}) \end{bmatrix} = 2\pi \int_\Gamma \begin{bmatrix} U_{rr}(\boldsymbol{\xi},\mathbf{x}) & U_{rz}(\boldsymbol{\xi},\mathbf{x}) \\ U_{zr}(\boldsymbol{\xi},\mathbf{x}) & U_{zz}(\boldsymbol{\xi},\mathbf{x}) \end{bmatrix} \begin{bmatrix} t_r(\mathbf{x}) \\ t_z(\mathbf{x}) \end{bmatrix} r_{\mathbf{x}} d\Gamma - 2\pi \int_\Gamma \begin{bmatrix} T_{rr}(\boldsymbol{\xi},\mathbf{x}) & T_{rz}(\boldsymbol{\xi},\mathbf{x}) \\ T_{zr}(\boldsymbol{\xi},\mathbf{x}) & T_{zz}(\boldsymbol{\xi},\mathbf{x}) \end{bmatrix} \begin{bmatrix} u_r(\mathbf{x}) \\ u_z(\mathbf{x}) \end{bmatrix} r_{\mathbf{x}} d\Gamma \quad (1)$$

where C_{rr}, C_{rz}, C_{zr} and C_{zz} are constants which depend on the geometry at $\boldsymbol{\xi}$, u_r and u_z are the radial and axial displacements, t_r and t_z are the radial and axial tractions, $\boldsymbol{\xi}$ is the point where the ring unit load is applied, $\mathbf{x}$ is the integrating field point and U and T are the axisymmetric displacement and traction kernels, respectively.

The displacement kernels are

$$U_{rr}(\boldsymbol{\xi},\mathbf{x}) = \left[\frac{(3-4\nu)\,C_1\left(r_\xi^2+r_{\mathbf{x}}^2\right)}{C_2 r_\xi r_{\mathbf{x}}} + \frac{4\,(1-\nu)\,C_1\,(z_\xi - z_{\mathbf{x}})^2}{C_2 r_\xi r_{\mathbf{x}}}\right] K_1\left(C_4, \frac{\pi}{2}\right) - \left[\frac{(3-4\nu)\,C_1 C_2}{r_\xi r_{\mathbf{x}}} + \frac{C_1\,(z_\xi - z_{\mathbf{x}})^2\left(r_\xi^2+r_{\mathbf{x}}^2+(z_\xi - z_{\mathbf{x}})^2\right)}{C_2 C_3 r_\xi r_{\mathbf{x}}}\right] K_2\left(C_4, \frac{\pi}{2}\right) \quad (2)$$

$$U_{rz}(\boldsymbol{\xi},\mathbf{x}) = \left[\frac{C_1\,(z_\xi - z_{\mathbf{x}})}{C_2 r_{\mathbf{x}}}\right] K_1\left(C_4, \frac{\pi}{2}\right) + \left[\frac{C_1\,(z_\xi - z_{\mathbf{x}})\left(r_\xi^2 - r_{\mathbf{x}}^2 - (z_\xi - z_{\mathbf{x}})^2\right)}{C_2 C_3 r_\xi}\right] \times K_2\left(C_4, \frac{\pi}{2}\right) \quad (3)$$

$$U_{zr}(\boldsymbol{\xi},\mathbf{x}) = \left[\frac{C_1\,(z_{\mathbf{x}} - z_\xi)}{C_2 r_\xi}\right] K_1\left(C_4, \frac{\pi}{2}\right) + \left[\frac{C_1\,(z_\xi - z_{\mathbf{x}})\left(r_\xi^2 - r_{\mathbf{x}}^2 + (z_\xi - z_{\mathbf{x}})^2\right)}{C_2 C_3 r_{\mathbf{x}}}\right] \times K_2\left(C_4, \frac{\pi}{2}\right) \quad (4)$$

$$U_{zz}(\boldsymbol{\xi},\mathbf{x}) = \left[\frac{(6-8\nu)\,C_1}{C_2}\right] K_1\left(C_4, \frac{\pi}{2}\right) + \left[\frac{2C_1\,(z_\xi - z_{\mathbf{x}})^2}{C_2 C_3}\right] K_2\left(C_4, \frac{\pi}{2}\right) \quad (5)$$

where r_ξ and $r_{\mathbf{x}}$ are the radial distances from the source and field points to the axis of symmetry, z_ξ and $z_{\mathbf{x}}$ are the axial coordinates, K_1 and K_2 are the complete elliptic integrals of the first and second kind and the constants C_1, C_2, C_3 and C_4 are defined by

$$\begin{aligned} C_1 &= \frac{(1+\nu)}{8\pi^2 E(1-\nu)} \\ C_2 &= \sqrt{(r_\xi + r_{\mathbf{x}})^2 + (z_\xi - z_{\mathbf{x}})^2} \\ C_3 &= (r_\xi - r_{\mathbf{x}})^2 + (z_\xi - z_{\mathbf{x}})^2 \\ C_4 &= \sqrt{\frac{4 r_\xi r_{\mathbf{x}}}{(r_\xi + r_{\mathbf{x}})^2 + (z_\xi - z_{\mathbf{x}})^2}} \end{aligned} \quad (6)$$

where E is the Young's modulus of elasticity, and ν the Poisson's ratio.

The expressions for traction kernels can be directly obtained from Hooke's law where they are written in terms of the previous displacement kernels and their derivatives,

$$T_{rr}(\boldsymbol{\xi},\mathbf{x}) = \frac{E}{(1+\nu)}\left[\frac{(1-\nu)}{(1-2\nu)}\frac{\partial U_{rr}}{\partial r}+\frac{\nu}{(1-2\nu)}\left(\frac{U_{rr}}{r}+\frac{\partial U_{rz}}{\partial z}\right)\right]n_r + \frac{E}{2(1+\nu)}\left(\frac{\partial U_{rr}}{\partial z}+\frac{\partial U_{rz}}{\partial r}\right)n_z \tag{7}$$

$$T_{rz}(\boldsymbol{\xi},\mathbf{x}) = \frac{E}{(1+\nu)}\left[\frac{(1-\nu)}{(1-2\nu)}\frac{\partial U_{rz}}{\partial z}+\frac{\nu}{(1-2\nu)}\left(\frac{U_{rr}}{r}+\frac{\partial U_{rr}}{\partial r}\right)\right]n_z + \frac{E}{2(1+\nu)}\left(\frac{\partial U_{rr}}{\partial z}+\frac{\partial U_{rz}}{\partial r}\right)n_r \tag{8}$$

$$T_{zr}(\boldsymbol{\xi},\mathbf{x}) = \frac{E}{(1+\nu)}\left[\frac{(1-\nu)}{(1-2\nu)}\frac{\partial U_{zr}}{\partial r}+\frac{\nu}{(1-2\nu)}\left(\frac{U_{zr}}{r}+\frac{\partial U_{zz}}{\partial z}\right)\right]n_r + \frac{E}{2(1+\nu)}\left(\frac{\partial U_{zz}}{\partial r}+\frac{\partial U_{zr}}{\partial z}\right)n_z \tag{9}$$

$$T_{zz}(\boldsymbol{\xi},\mathbf{x}) = \frac{E}{(1+\nu)}\left[\frac{(1-\nu)}{(1-2\nu)}\frac{\partial U_{zz}}{\partial z}+\frac{\nu}{(1-2\nu)}\left(\frac{U_{zr}}{r}+\frac{\partial U_{zr}}{\partial r}\right)\right]n_z + \frac{E}{2(1+\nu)}\left(\frac{\partial U_{zz}}{\partial r}+\frac{\partial U_{zr}}{\partial z}\right)n_r \tag{10}$$

where n_r and n_z are the unit normal components at $\mathbf{x}$. Expanded expressions for the traction kernels are quite lengthy (Becker, 1986) and their numerical evaluation demands an accurate computation of the elliptic integrals (Abramowitz & Stegun, 1965).

At first glance, one may think that when the source point lies on the axis of symmetry a singularity appears since $r_\xi \to 0$. However, expanding the kernels U and T, and then simplifying, expressions identical to the 3-D ones are obtained, as expected.

The BEM basically consists on discretizing the boundary of the domain with elements of certain geometry which contain nodal points. In the present problem these points represent either unknown or prescribed (usually two of them) nodal values of displacements and tractions. An appropriate choice of interpolating functions allows the computation of these values at other parts of the element.

Equation (1) is applied at each nodal point according to the boundary discretization. A discretized system of equations is obtained where integrals of the kernels U and T over each element must be computed. Two types of integrations will appear: non-singular and singular. The first ones are straightforward (Gauss quadrature) and the second require different treatments depending on which kernel is being integrated. The singular behaviour of kernel U is similar to the 2-D one. Normal integration is carried out except for the singular logarithmic term, embedded in the elliptic function K_1, which is integrated with Gauss-Log quadrature. Improper integrals of kernel T plus the coefficients C_{rr}, C_{rz}, C_{zr} and C_{zz} are calculated combining two techniques: rigid body movement along the z

axis and a particular choice of stress conditions applicable to any type of problem (Becker, 1986).

A fully-populated system of equations $\mathbf{Sy} = \mathbf{b}$ is finally obtained where $\mathbf{y}$ contains the unknown boundary values of displacements and tractions in directions r and z, $\mathbf{S}$ is the coefficients matrix where each term corresponds to an element integration and $\mathbf{b}$ is the independent vector resulting from the multiplication of integrated terms by associated prescribed values.

3. CONTACT PROBLEM AND IMPLEMENTATION

Consider a non-conforming type of contact (Fig. 1) between two axisymmetric elastic bodies subject to external loads and constraints. Compressive and shear forces are transmitted through the contact area setting the whole system in equilibrium. Particularly, in cases where friction is negligible, tangential (shear) stresses are equal to zero. The final extent of the contact area is not known *a priori* and depends on the magnitude of the applied external forces. This load dependence of the problem makes it nonlinear and an iterative procedure is required for its solution. Furthermore, the presence of friction implies the development of shear stresses whose magnitudes may lead to relative tangential displacements at the contact interface. Therefore, for the correct evaluation of these stresses, it is necessary to have the external loads applied incrementally.

In a contact problem at least two bodies are involved and their boundaries can be subdivided into non-contact areas and potential contact areas, as shown in Fig. 1b. The non-contact areas, after discretization, are conventionally composed by nodes with two prescribed values and two unknowns each. On the other hand, the potential contact areas (name given since the area of contact is not known *a priori*) are discretized matching the nodal points of each contacting body, forming contact node pairs with 8 unknown variables each (u_r, u_z, t_r and t_z for each node). The discretized boundary integral equation (1) is applied twice (two directions) in each nodal point of the system so an extra 4 equations for each contact node pair is necessary to have a well-defined mathematical formulation. These extra contact equations must account for the equilibrium and continuity conditions between bodies at the contact interfaces.

At any step of the load incrementation history the potential contact area is formed by two zones: the separated contact zone and the effective contact zone. Node pairs in the first zone are separated while in the second they are joined. The second zone increases as the load increases and may also be partitioned into slip and stick (friction must exist) regions. Given a load step, the slip region is composed by contact node pairs that have experienced a relative tangential displacement while at the stick region node pairs have not experienced the same sort of relative displacement. At each load step a new configuration for the potential contact area will exist and a different group of contact equations must be applied. The set of additional equations for each node pair (*e.g.* pair ab), depending on its contact condition status, is shown in table 1 where n and t are the local normal and tangential directions at the contact nodes and μ is the friction coefficient.

Table 1. Contact Equations

	Status		
Equations	separate	slip	stick
Equilibrium	$t_t^a - t_t^b = 0$ $t_n^a - t_n^b = 0$	$t_t^a - t_t^b = 0$ $t_n^a - t_n^b = 0$	$t_t^a - t_t^b = 0$ $t_n^a - t_n^b = 0$
Compatibility	$t_t^a = 0$ $t_n^a = 0$	$t_t^a \pm \mu t_n^a = 0$ $u_n^a + u_n^b = 0$	$u_t^a + u_t^b = 0$ $u_n^a + u_n^b = 0$

In a non-conforming contact problem the initial configuration is simply an effective contact zone defined by a point and zero applied loads. When the load is applied and gradually increased the point contact becomes an area of contact whose typical characteristic is a boundary with slipping traction conditions in the vicinity of a separated zone with traction free conditions, as observed by Hertz (1896). Once the discretization is introduced the contact interface is represented by several linear elements and contact node pairs. One of these pairs will represent the initial point contact configuration and by incrementing the load other pairs will join. The most desirable situation is to have, at any load step, a pair of nodes at the edge of the effective contact area in order to guarantee proper traction continuity. However, the nonlinear relation between load and contact area makes it impossible to foresee the necessary load increments, so to accomplish this requirement, the fully incremental loading technique is implemented. The basic idea of this technique is to use a linear extrapolation function to obtain a very close to zero normal traction value at the edge of the effective contact area.

Consider a pair of linear contact elements formed by two contact node pairs at its edges. One of the node pairs is joined at the edge of the current contact area and the other pair is the next one to be joined once the load is incremented. The applied load at this stage is αP $(0 < \alpha < 1)$ and the necessary increment ΔP for this task is required. The second pair of nodes is set to slip contact conditions, the new edge of the contact area. Initially, an arbitrary load βP $(\beta > \alpha)$ is applied and a normal traction value t_n^1 is obtained. Afterwards, another arbitrary value γP $(\gamma > \beta)$ is applied to produce t_n^2. Using these values and an extrapolation formula the required load increment to achieve t_n very close to zero can be calculated from $\Delta P = (\delta - \alpha)P$ where

$$\delta = \beta + (\gamma - \beta)\frac{t_n^1}{t_n^1 - t_n^2} \tag{11}$$

A single application of this procedure is usually sufficient to get $t_n \cong 0$, unless the discretization is not refined enough. Another particularity is that for every different load value ($\beta P, \gamma P$ or δP), only the independent vector of the system of equations is changed. Therefore, using an LU solver, once the system decomposition is made, just the backsubstitution phase needs to be repeated to solve the system for each trial load.

The number of incremental load steps is equal to the number of contact elements to be joined. The higher the number of contact elements the smaller the load increments, the better the accuracy and longer the computational time. At each step different contact equations apply and a new LU decomposition is necessary. Performing this task for each step is very expensive. However, provided the number of changed contact equations at every step is very small compared to the number of equations in the system (that is the case since just one element per step is brought into contact) a special scheme to obtain the system solution for the new configuration, based on the Sherman-Morrison-

Woodbury formula (Press *et al.*, 1992), can be employed. Ezawa *et al.* (1989) used this solution method very efficiently in a similar type of contact analysis.

As mentioned before, a stick-slip partition may exist in the effective contact area depending on the friction and tangential traction values. At the end of every load step, new contact traction values will develop and tests must be performed to check whether the assumed contact status at the beginning of the load step is still valid at the end of the load step. If not, the contact status is corrected and the iteration step repeated. The following violation test for every new solution is applied to all contact node pairs,

	$gap^{ab} = gap_i^{ab} - (u_n^a + u_n^b)$
separation	> 0
joined	≤ 0

(12)

	$\lvert t_t \rvert$
stick	$< \lvert \mu t_n \rvert$
slip	$\geq \lvert \mu t_n \rvert$

(13)

where gap^{ab} is the normal gap at the contact pair ab and gap_i^{ab} is the initial one.

The iteration process terminates if either all contact node pairs have already joined or the total applied load is greater than the prescribed one.

4. COATED BEARING ANALYSES

Consider a ceramic coated steel bearing of radius $R = 12.7mm$ and variable coating thickness w in contact with a steel cylindrical foundation of radius $4R$ and height $6R$, as shown in Fig. 2. A vertical load P is applied at the top of the bearing, along its axis of symmetry, compressing it against the cylinder. The steel properties are defined by $E_s = 207GPa$ and $\nu_s = 0.3$.

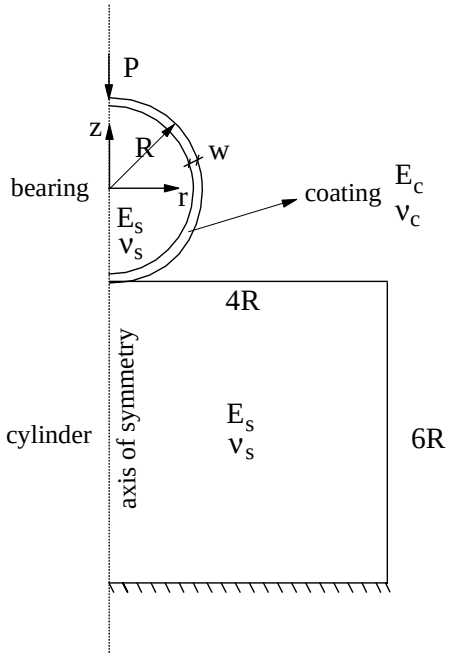

Figure 2: Coated bearing over an elastic cylinder.

In order to validate the formulation this problem is initially analysed without friction or coating and compared to analytical results. Stress values at the cylinder along the axis of symmetry and close to the contact area are shown in Fig. 3 for a load $P = 128.3N$. An excellent agreement with the Hertzian solution is achieved, with a relative error generally smaller than 1.0%. At the left side of Fig. 4 the computed results for the normal pressure along the contact area for several load steps, up to $P = 128.3N$, are plotted. The results for the last step are also successfully compared to the analytical ones. At the right side of Fig. 4 the same analysis is performed with friction $\mu = 0.01$. It is interesting to observe that normal traction values are not different from those from the frictionless case, as well as the growth of tangential tractions with the increasing load. In this particular case no slip regions were developed in the contact area despite the small friction value.

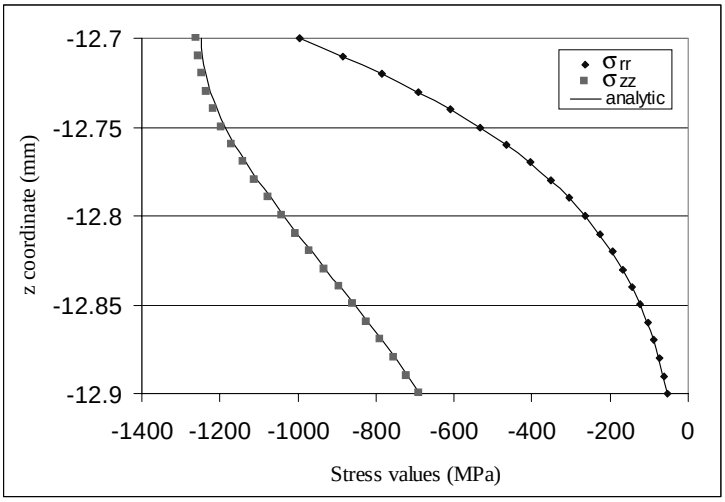

Figure 3: Stresses in Hertzian problem

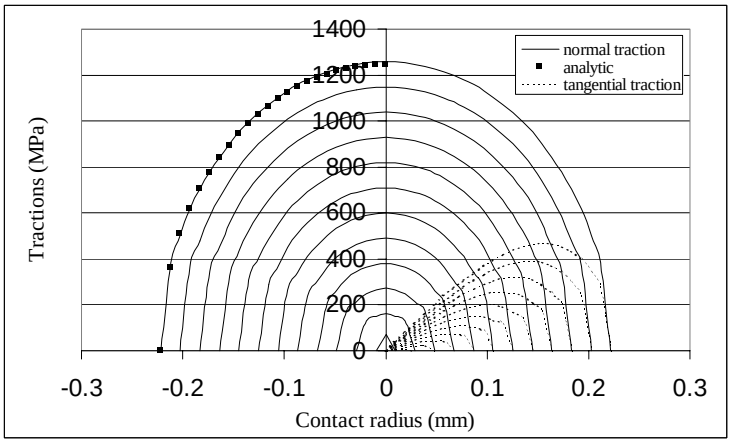

Figure 4: Normal and tangential tractions growth in the contact area

Three coating thicknesses ($w1 = 0.1mm$, $w2 = 0.2mm$ and $w3 = 0.4mm$) and two different ceramic materials ($a)E_c = 2E_s$ and $b)E_c = 4E_s$; $\nu_c = 0.3$) were employed in the

next set of analyses. The bearing was pressed against the cylinder until a contact area of radius $0.202mm$ was formed. Stress values at the bottom of the bearing along the axis of symmetry are compared in Figs. 5 and 6 for several combinations of coating properties. Only σ_{rr} and σ_{zz} are plotted since at the axis z the shear stress $\tau_{rz} = 0$ and the hoop stress $\sigma_{\theta\theta} = \sigma_{rr}$.

It can be seen in Fig. 5 that the normal stress values σ_{zz} are consistent for all cases. The less rigid bearing without coating ($w0$) has smaller stress values while the most rigid one ($w3b$) has higher values. The same pattern is observed when comparing bearings of same coating thickness but different elasticity modulus.

In Fig. 6 σ_{rr} is plotted for three bearings with same material but different coating thicknesses. The results are compared to the zero coating case and higher stress values are obtained. As expected, σ_{rr} presents a discontinuity at the coating/substrate interface.

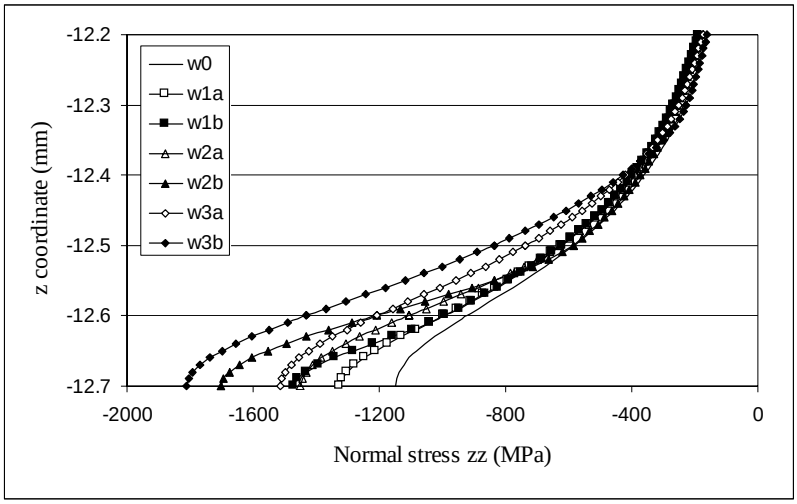

Figure 5: σ_{zz} along the axis of symmetry at the bottom of the bearing

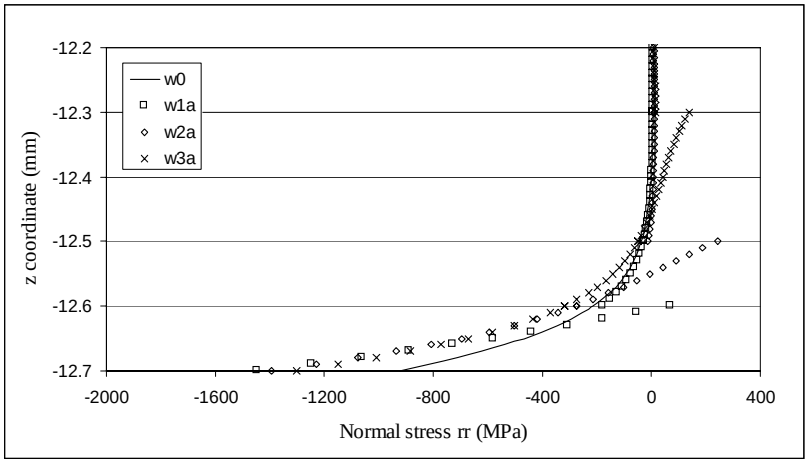

Figure 6: σ_{rr} along the axis of symmetry at the bottom of the bearing

5. CONCLUSIONS

A boundary element formulation has been developed for the investigation of contact stresses in layered axisymmetric bodies. A fast solver routine and the fully incremental loading technique were implemented to speed up the analysis and guarantee proper traction behaviour at the edge of the contact area, respectively.

Results from the analysis of homogeneous bodies compared very well with analytical solutions. Coulomb friction was introduced and the development of tangential tractions was observed. Different coatings over a steel bearing were analysed and consistent stress values near the contact zone were obtained.

REFERENCES

Hertz, H., 1896, Miscellaneous papers - On the Contact of Elastic Solids (translated by D. E. Jones), Macmillan, London.

Abramowitz, M. and Stegun, I. A., 1965, Handbook of Mathematical Functions, Dover, New York.

Chen, W. T., 1971, Computation of stresses and displacements in a layered elastic medium, International Journal of Engineering Science, vol. 9, pp. 775-800.

Gupta, P. K. and Walowit, J. A., 1974, Contact stress between an elastic cylinder and a layered elastic solid, Transactions of the ASME, Journal of Lubrication Technology, pp. 250-257.

Abdul-Mihsein, M. J., Bakr, A. A. and Parker, A. P., 1986, A boundary integral equation method for axisymmetric elastic contact problems, Computers and Structures, vol. 23, n. 6, pp. 787-793.

Becker, A. A., 1986, The Boundary Integral Equation Method in Axisymmetric Stress Analysis Problems, Springer-Verlag, Berlin.

Ezawa, Y. and Okamoto, N., 1989, High-speed boundary element contact stress analysis using a supercomputer, Proceedings of the Boundary Element Techniques: Application in Engineering, Computational Mechanics Publication, Southampton.

Press, W. H., Teukolsky, S. A., Vertterling, W. T. and Flannery, B. P., 1992, Numerical Recipes in Fortran, Cambridge University Press, Cambridge.

Djabella, H. and Arnell, R. D., 1992, Finite element analysis of the contact stress in an elastic coating on an elastic substrate, Thin Solid Films, vol. 213, pp. 205-219.

Man, K. W., Aliabadi, M. H. and Rooke, D. P., 1993, BEM frictional contact analysis: modelling considerations, Engineering Analysis with Boundary Elements, vol. 11, n. 1, pp. 77-85.

Schwarzer, N., Djabella, H., Richter, F. and Arnell, R. D., 1995, Comparison between analytical and FEM calculations for the contact problem of spheric indentors on layered materials, Thin Solid Films, vol. 270, pp. 279-282.

Ahmed, R., 1997, Rolling Contact Fatigue of Thermal Spray Coatings, Ph.D. thesis, Department of Mechanical Engineering, Brunel University, UK.